RESEARCH ARTICLE | MARCH 03 2025

Impact of biased cooling on the operation of undoped silicon quantum well field-effect devices

Laura K. Diebel ; Lukas G. Zinkl ; Andreas Hötzinger ; Felix Reichmann ; Marco Lisker ; Yuji Yamamoto ; Dominique Bougeard

AIP Advances 15, 035301 (2025)
https://doi.org/10.1063/5.0250968

Impact of biased cooling on the operation of undoped silicon quantum well field-effect devices

Cite as: AIP Advances 15, 035301 (2025); doi: 10.1063/5.0250968
Submitted: 28 November 2024 • Accepted: 10 February 2025 •
Published Online: 3 March 2025

Laura K. Diebel,[1] Lukas G. Zinkl,[1] Andreas Hötzinger,[1] Felix Reichmann,[2] Marco Lisker,[2] Yuji Yamamoto,[2] and Dominique Bougeard[1,a)]

AFFILIATIONS

[1] Fakultät für Physik, Universität Regensburg, 93040 Regensburg, Germany
[2] IHP—Leibniz-Institut für innovative Mikroelektronik, 15236 Frankfurt (Oder), Germany

[a)] Author to whom correspondence should be addressed: dominique.bougeard@ur.de

ABSTRACT

Gate-tunable semiconductor nanosystems are getting more and more important in the realization of quantum circuits. While such devices are typically cooled to operation temperature with zero bias applied to the gate, *biased cooling* corresponds to a non-zero gate voltage being applied before reaching the operation temperature. We systematically study the effect of biased cooling on different undoped SiGe/Si/SiGe quantum well field-effect stacks designed to accumulate and density-tune two-dimensional electron gases (2DEGs). In an empirical model, we show that biased cooling of the undoped FES induces a static electric field, which is constant at operation temperature and superimposes onto the field exerted by the top gate onto the 2DEG. We show that the voltage operation window of the field-effect-tuned 2DEG can be chosen in a wide range of voltages via the choice of the biased cooling voltage. Importantly, quality features of the 2DEG such as the mobility or the temporal stability of the 2DEG density remain unaltered under biased cooling.

I. INTRODUCTION

Field-effect devices are an important building block for the realization of quantum circuits in semiconductor heterostructures,[1–6] in particular since they offer a gate-tunability of electric carriers down to the nanoscale. It becomes more and more clear that a precise understanding of the electrostatics created by gate tuning in semiconductor heterostructure field-effect stacks (FESs) is highly relevant for the stable operation of quantum circuits.[7–14] Typically, FESs are cooled down with zero bias applied to the gates. *Biased cooling* represents the cool-down under a non-zero applied gate voltage. Biased cool-down has been studied for modulation-doped GaAs/AlGaAs quantum well (QW) heterojunctions in the context of the operation of two-dimensional electron gases (2DEGs)[15–18] and of quantum point contacts.[19,20] In these works, the observed impact on the operation of the devices has been phenomenologically linked to the presence of dopant-induced defects and to leakage of Schottky gates. The statistical nature of dopant-induced defects and of the presence of leakage has limited the application of biased cooling as an additional degree of freedom for the device operation. More recently, in particular for spin qubit quantum circuits, FES based on undoped semiconductor heterostructures and including oxide-based dielectrics instead of Schottky gates are used.[14,21,22] The absence of dopant-induced defects and the dielectric/semiconductor interface in the FES create an electrostatic environment in which biased cooling has only recently started to be considered in a report of biased cooling-dependent shifts of the turn-on voltage in a single electron transistor device.[23]

In this paper, we systematically study the effect of biased cooling on different undoped SiGe/Si/SiGe QW FESs. We show that biased cooling with a voltage U_{BC} induces a static electric field within the FES. At the operation temperature of the device, here 1.5 K, this static electric field is independent of the top gate voltage U_{TG} and overlays the action of U_{TG} on the 2DEG. As a result, the accumulation voltage of the 2DEG, as well as the whole field-effect tuning range of the 2DEG density n_e, can be deterministically shifted to a chosen voltage range by the appropriate choice of U_{BC}. Notably, shifting the 2DEG operation range does not impact 2DEG quality markers such as the electron mobility and the temporal stability of the 2DEG density. In an empirical model, we show that the charge density that induces the static electric field is localized at the dielectric/heterostructure interface of the FES. These observations remain valid for FES with and without a Si cap at the interface to the dielectric.

II. FIELD-EFFECT STACKS AND EXPERIMENTAL SETUP

We investigated the biased cooling effect on three different undoped Si/SiGe FESs capable of hosting a 2DEG. These FESs are standard undoped $Si_{1-x}Ge_x/Si/Si_{1-x}Ge_x$ quantum well heterostructures for field-effect applications.[21,24,25] All of them share the same functional layer structure shown in Fig. 1, but with some crucial differences summarized in Table I. One of the key differences to highlight is the absence of a Si cap on FES A. FES A was grown and fabricated at the *IHP—Leibniz-Institut für innovative Mikroelektronik*,[26] whereas the FESs B and C were both grown and fabricated at the *Universität Regensburg*.[8] FES B and C possess a 1.5 nm thick Si cap, naturally oxidized in air. The characterization of the FESs was performed by Hall-bar geometry magneto-transport measurements at a temperature of 1.5 K using standard lock-in techniques with a Hall-bar current of 50 nA. The voltage applied at the top gate (TG) is denoted U_{TG}.

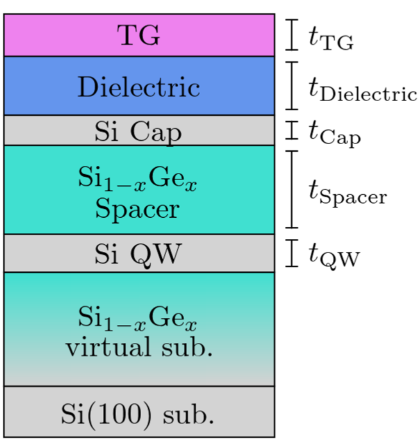

FIG. 1. Cross section schematic of the undoped Si/SiGe FESs. Details on the investigated FES A, B, and C are listed in Table I.

TABLE I. Overview of the three undoped SiGe/Si/SiGe quantum well FES A, B, and C. The abbreviations are introduced in Fig. 1.

FES	A	B	C
Dielectric (method)	SiOx (HDP)	AlOx (ALD)	AlOx (ALD)
TG	TiN	Ti/Au	Ti/Au
t_{TG} (nm)	30	10/100	10/100
$t_{Dielectric}$ (nm)	10	20	50
t_{Cap} (nm)	0	1.5	1.5
t_{Spacer} (nm)	33	45	45
t_{QW} (nm)	7	12	12
x	0.34	0.26	0.32
Heterostructure growth	CVD	MBE	MBE

III. RESULTS

A. Impact of biased cooling on the 2DEG characteristics

We find the heterostructures in all three FESs to be conducting at room temperature for any U_{TG} value, even at U_{TG} = 0 V. On the contrary, we observe the conductance of the heterostructure to freeze out during the cool-down to 1.5 K, stating that the 2DEGs are normally off at U_{TG} = 0 V. To explore the influence of the biased cooling on the transport properties of a 2DEG, we apply a non-zero voltage at the TG while cooling down the field-effect stacks from room temperature to 1.5 K. We refer to this voltage applied during the cool-down as *biased cooling voltage* U_{BC}. We cooled down the FES various times with varying U_{BC} and determined the electron density as a function of the applied TG voltage (U_{TG} sweep) at 1.5 K for each cool-down. These measurements were performed for all three FES A, B, and C. Figure 2(a) representatively displays the results for FES A, while the corresponding results for FES B and FES C are provided in the supplementary material. The FESs cooled down with the commonly used U_{BC} = 0 V, showing 2DEG accumulation in the Si QW at a positive U_{TG}. In the classical approximation of a capacitor where the 2DEG and the TG are the plates, the electron density n_e of the 2DEG within the QW depends linearly on the voltage U_{TG} applied at the TG. This approximation starts to break down as soon as the potential difference is strong enough for electrons to tunnel out of the QW, through the SiGe barrier, into the interface between the heterostructure and the dielectric. In this saturation regime, the n_e does not further increase with U_{TG}.[27–30] As seen in Fig. 2(a), we find this characteristic behavior of a linear increase of n_e, followed by a saturation, to be independent of the applied U_{BC}. In quantum Hall experiments for selected negative and positive U_{BC}, we have verified that the electron density contributing to the transport after cooling down with a non-zero U_{BC} is exclusively located in the QW 2DEG, excluding measurable, biased cooling-induced parallel conductance. Comparing the electron density curves, we observe a shift induced by U_{BC}. For positive biased cooling voltages applied during the cool-down, the electron density curves shift toward more positive/higher U_{TG}, whereas for negative biased cooling, they shift toward more negative/lower U_{TG}. The shift increases with the absolute value of the U_{BC} applied during cool-down.

In the remainder of this paper, we focus on the linear electron density tuning regime, which is the operation region for most field-effect device applications, including quantum circuits. We have verified that the 2DEG densities n_e are reproducible within cool-downs in all three FESs (no hysteresis of the electron density in a U_{TG} sweep). They are also reproducible among separate cool-downs for a given U_{BC} value. As a lower bound for the operation region, we define the current in the Hall bar as reaching 48 nA. We have verified that all three FES features accumulated 2DEGs at this current value. We denote $n_{e,lb}$ the lower bound density and U_{Acc} the

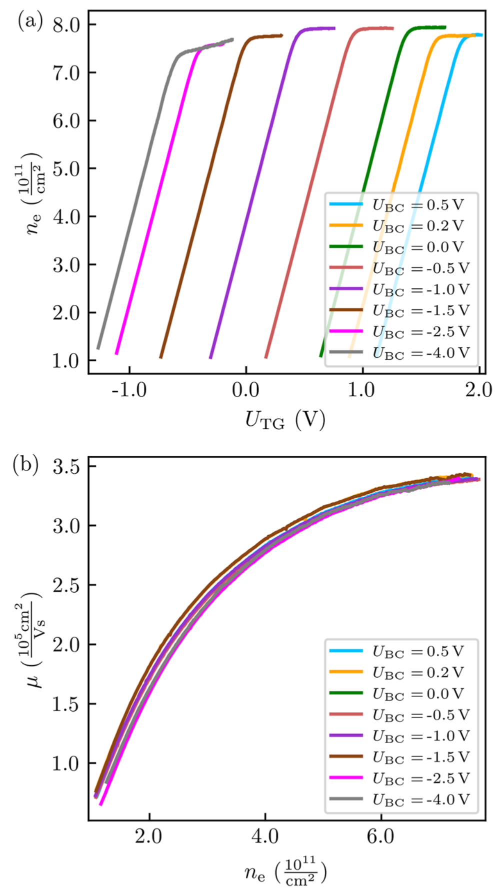

FIG. 2. Impact of biased cooling on the electron density and the mobility of the 2DEG, representatively shown for FES A at 1.5 K. The definitions of the different voltages and of $n_{e,ub}$ are found in the text. (a) 2DEG density n_e as a function of U_{TG} for different biased cooling voltages U_{BC}. (b) 2DEG mobility μ dependence on n_e within the linear capacitive coupling regime ($n_e < n_{e,ub}$) for different biased cooling voltages U_{BC}.

corresponding top gate voltage. Analyzing the lower bound electron density at U_{Acc} for the different U_{BC}, we see an average value of $n_{e,lb} = 1.1\times10^{11}$ 1/cm^2 for FES A in Fig. 2(a). We define the upper bound electron density $n_{e,ub}$ of the linear operation regime as the end of this range by extracting the first n_e value that deviates by 2% from a linear fit of the data. For FES A we evaluate the average value of the upper bound electron density to be $n_{e,ub} = 7.5\times10^{11}$ 1/cm^2. Across all FES, we observe no systematic dependence of the lower bound electron density $n_{e,lb}$ as well as of the upper bound electron density $n_{e,ub}$ on U_{BC}. In addition, the slope of the 2DEG density's U_{TG}-dependence—which represents the capacitive coupling between the TG and the 2DEG—is unaffected by biased cooling with $U_{BC} \neq 0$ V for all three FESs [see Fig. 2(a) representatively for FES A]. In Fig. 2(b), we report the 2DEG mobility μ as a function of n_e for all tested U_{BC}, representatively for FES A. No impact of U_{BC} on the μ is observed. Note that remote scatterers should particularly manifest in the region of steep mobility increase below circa $n_e < 4\times10^{11}$ 1/cm^2 in FES A, while scatterers in the QW will dominate beyond.[30,31]

To summarize the key features observed for the three FESs and representatively shown for stack A in Fig. 2: The main consequence of the biased cooling effect is a shift of the field-effect tuned 2DEG density compared to $U_{BC} = 0$ V, the shift increasing with the absolute value of U_{BC}. At the same time, the U_{TG}-tunable n_e range, the capacitive coupling between the TG and the 2DEG, and the μ at each given n_e are unaffected by U_{BC}. Finally, the heterostructures are conductive at room temperature, while this conductivity vanished during the cool-down. At this point it should be highlighted that these observations are identical in all three FESs, although they differ with respect to the presence of a Si cap, the dielectric material and its thickness, as well as in the epitaxy method of the heterostructures (CVD vs MBE), their Ge content, and the thicknesses of the SiGe barrier (see Fig. 1 and Table I).

A plausible source for the observed experimental phenomenology is an additional static U_{BC}-dependent electric field, which superimposes onto the field resulting from U_{TG} at the QW at 1.5 K. The charge causing this static field needs to be adjustable by the applied U_{BC} at room temperature to explain the U_{BC}-dependent shift of the accumulation voltage U_{Acc}. At the same time, to guarantee the observed parallel shift—i.e., constant capacitive coupling—of the U_{TG} sweeps in Fig. 2(a), this charge must be independent of U_{TG} at 1.5 K.

Since we verified via quantum Hall traces that no measurable parallel conductance channel occurs at 1.5 K after cooling down with $U_{BC} \neq 0$ V, i.e., that transport occurs solely within the 2DEG, this additional charge must be immobile under device operation at 1.5 K. In case this hypothetical charge would build-up in the vicinity of the QW after cooling down with $U_{BC} \neq 0$ V, we would expect a variation in the potential fluctuations affecting the 2DEG in correlation to U_{BC}.[31] As we experimentally find the 2DEG mobility at higher 2DEG densities [Fig. 2(b)] and also the lower bound 2DEG density $n_{e,lb}$ [Fig. 2(a)] to be unaffected by U_{BC} in all three FESs, we conclude that the charge build-up occurs further away from the QW and is homogeneously distributed. Given that the SiGe barrier is undoped, the most plausible locations are the thin Si cap and the heterostructure interface with the polycrystalline dielectric oxide. As FES A, in contrast to B and C, does not contain a Si cap but shows the same behavior under the influence of biased cooling, we exclude the necessity of a Si cap for this effect. Hence, from the previously acquired requirements, we conclude that the charges induced at room temperature by the U_{BC} are localized at the interface between the heterostructure and the polycrystalline dielectric. This interface meets all the criteria. It has been previously shown to host a large enough density of trap states to allow for charge build-ups up to a screening of the capacitive coupling between the TG and the 2DEG.[27–30] Its location in between the TG and the QW allows the electric field of the trapped interface charges to statically superimpose the electric field of the TG effectively, without being too close to the QW to influence the 2DEG mobility and the lower bound 2DEG density. We have verified in 1D Schrödinger-Poisson simulations that the introduction of a fixed charge density at the dielectric/heterostructure interface allows us to mimic the experimental behavior reported in Fig. 2(a). The required charge density is of the order of 10^{11} 1/cm^2, in accordance with reports on charge traps[27–30] and capacitance-voltage estimations for the oxide used in FES A. Since all three heterostructures are conductive at room temperature, positive as well as negative U_{BC} may induce the hypothetical charges exerting the static electric field by loading or unloading trap states at the interface. On the contrary, the freeze out of the conductance of the heterostructure during the cooldown to 1.5 K suppresses this loading mechanism of interface trap states.

B. Empirical model for biased cooling of undoped QW heterostructures

Based on this hypothesis, we develop a model for the biased cooling effect in the following. Our model relies on the fact that the top gate and the interface between the heterostructure and the dielectric act like a classical capacitor at room temperature. Essential ingredients of the model are sketched in Fig. 3. The mechanism for loading and unloading the interface at room temperature—and hence before the freeze out of the heterostructure—is sketched in Fig. 3(a). Panel 3(a-i) shows the conductance band edge energy of the heterostructure stack (dark red line) for $U_{\mathrm{BC}} = 0$ V, with the ground state energy of the Si QW depicted in black. For simplicity, we illustrate this reference case with a flat band edge. These interface states (sketched as red circles) are populated up to the Fermi energy (blue dashed line) with electrons (magenta dots). A non-zero applied U_{BC} at the TG results in a tilt of the band edge in the sketches. In the case of a $U_{\mathrm{BC}} < 0$ V, this lifts a certain amount Q of occupied interface states above the Fermi energy (non-equilibrium situation) shown in panel 3 (a-ii). Due to the room temperature conductivity of the FES, these electrons will, however, quickly unload from the interface. This results in a less negative/more positive charge configuration at the interface. As a consequence, two properties of the classical capacitor formed by the top gate and the dielectric/heterostructure interface manifest, as sketched in panel 3 (a-iii): First, the band bending between the top gate and the interface steepens in the dielectric compared to panel 3 (a-ii) proportionally to the charge reconfiguration. Second, outside of the capacitor—i.e., below the interface (in the heterostructure)—there is no electric field. Hence, the conduction band is flat again, as in panel 3 (a-i). In exact analogy, for $U_{\mathrm{BC}} > 0$ V, the applied electric field leads to pushing unoccupied interface states containing Q charges below the Fermi energy [see panel 3 (a-iv)] in non-equilibrium. The charge reconfiguration resulting from the room temperature conductivity of the FES hence adds the amount Q of electrons to the interface [see Fig. 3(a-v)]. Therefore, we end up in a more negative charge configuration at the interface compared to panel 3 (a-i). The model in Fig. 3(a) highlights two features, which are key to explain the experimental observations: The applied U_{BC} changes the charge state at the interface. In addition, the energetic position of the TG relative to the QW ground state energy

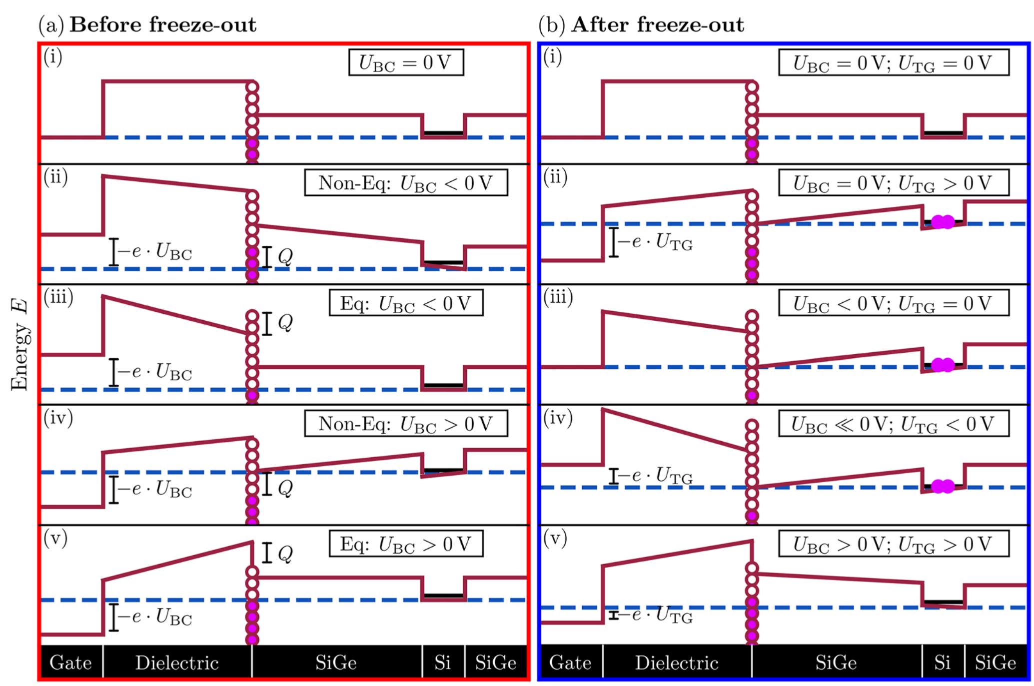

FIG. 3. Empirical model of the biased cooling effect. The panels (i–v) in (a) and (b) are discussed in detail in the text. The dark red line depicts the conduction band edge for different regions of the gate stack indicated at the bottom of the figure. The black line within the Si represents the confined ground state energy of the QW. We chose to fix the lower end of the QW conduction band energy at 0 V. The blue dashed line illustrates the Fermi energy. The empty red circles between the dielectric and the SiGe depict empty trap states at the dielectric/heterostructure interface. Electrons are shown as magenta colored dots and can fill these states at the interface. (a) Impact of U_{BC} applied before freeze out of the heterostructure. At these temperatures, the heterostructure is conductive. Each panel (i)–(v) illustrates a distinct equilibrium or non-equilibrium for specific U_{BC} situations. The charge Q results from electrons, which are loaded to or unloaded from the interface due to the applied U_{BC}. (b) Impact of U_{BC} after freeze out of the conductivity of the heterostructure. At the typical device operation temperature of 1.5 K, the electrons at the interface then cannot be loaded or unloaded anymore. Each panel (i)–(v) illustrates a specific scenario of the combination of U_{BC} and U_{TG}. Electrons within the Si QW illustrate the accumulation of the 2DEG.

changes as a function of the applied U_{BC}, while flat band conditions are retained between the interface and the QW. Note that both features result from the fact that the top gate and the dielectric/heterostructure interface behave like the plates of a classical capacitor before freeze out.

Moving now to temperatures cold enough to freeze out the conductance of the heterostructure, a major consequence for our model is the suppression of loading or unloading of the trap states at the interface via the heterostructure. Hence, the charges Q trapped at the interface states before cool-down are not modified by variations of U_{TG} applied after freeze out. Figure 3(b-i), as a reference, shows the scenario of a FES that was cooled down with $U_{BC} = 0$ V, keeping $U_{TG} = 0$ V after freeze out. The charge density at the interface is non-zero, and the QW ground state is above the Fermi energy. Hence, no electrons are accumulated in the QW. In order to accumulate electrons within the QW, it is necessary to apply a positive U_{TG} strong enough to drag the QW ground state below the Fermi energy, as illustrated in panel 3 (b-ii). Importantly, since the interface states cannot be loaded after freeze out, the empty interface states pushed below the Fermi level will stay unoccupied, leaving the electric field induced by the electrons trapped at the interface unaffected by U_{TG} variations. The electron accumulation in the QW is sketched as magenta dots. The density of accumulated electrons in the 2DEG located in the QW is proportional to U_{TG}, experimentally resulting in the typical FES electron density curve shown for $U_{BC} = 0$ V in Fig. 2(a). Next, Fig. 3(b-iii) illustrates the case of a negative U_{BC}. Compared to $U_{BC} = 0$ V, the diminished electron density at the interface leads to a less negative electric field superimposing the field created by U_{TG}. This is visible as an additional downward tilt of the conduction band. The tilt drags the QW ground state closer to the Fermi energy. Now, a less positive U_{TG} (e.g., $U_{TG} = 0$ V) is required to accumulate electrons within the QW, in line with the electron density curves being shifted toward more negative U_{TG} in the experiment, as observed in Fig. 2(a). For even stronger negative U_{BC} applied during cool-down, Fig. 3(b-iv) illustrates the ability to already accumulate electrons in the QW at negative U_{TG}, capturing the experimental observation that the electron density curves are shifted even further toward negative U_{TG}. Figure 3(b-v) shows the opposite scenario of a positive U_{BC} applied during the cool-down. The increased electron density at the interface causes a stronger shielding of the U_{TG} compared to $U_{BC} = 0$ V, resulting in the experimentally observed shift of the electron density curves toward more positive U_{TG} [see Fig. 2(a)].

Summarizing our experimental observations and the empirical model, applying U_{BC} at room temperature traps an amount of charges $Q = C_{BC} \cdot U_{BC}$ at the dielectric/heterostructure interface [see Figs. 3(a-ii)–3(a-v)], where C_{BC} is the capacitive coupling between the TG and the conductive heterostructure during biased cool-down, before freeze out. After freeze out, the charge trapping mechanism is suppressed, turning Q into being insensitive to variations of U_{TG} (applied to the FES at 1.5 K). The constant, static electric field created by the trapped charges $Q(U_{BC})$ then superimposes the field imposed with a U_{TG} sweep [see Fig. 3(b)]. This is equivalent to stating that the accumulation voltage U_{Acc} of the 2DEG will be shifted exactly by U_{BC} with respect to $U_{BC} = 0$ V. As a consequence, our model predicts a linear relationship between $\Delta U_{Acc} = U_{Acc} - U_{Acc,U_{BC}=0\text{ V}}$ and U_{BC}, with a slope $s = 1$. In Fig. 4, we test this prediction by displaying ΔU_{Acc} for all three FESs. The linear relationship is indeed verified in a significant range of U_{BC}. In addition, the slopes s are only slightly smaller than 1, with $s = 0.9$ V/V for FES A and C and $s = 0.8$ V/V for FES B. This slight deviation seems to indicate that C_{BC} is a bit smaller than the capacitive coupling at 1.5 K. As a second feature of Fig. 4, we observe a deviation from the linear relationship beyond a certain negative value of U_{BC}. This suggests that the amount of interface states per energy interval decreases for larger negative U_{BC} and, therefore, lower energies in Fig. 3(b). Hence, fewer charges are unloaded from trap states at the interface at room temperature for these U_{BC}. Note that FES A does not include a Si cap, while FES B and C do, and that they were fabricated at different facilities with different fabrication methods and dielectrics. Both the deviation from linearity of ΔU_{Acc} and the slight variation of the capacitive coupling between 1.5 K and warmer temperatures (slope $s < 1$) thus seem to sensitively depend on non-systematic and subtle details of the FES fabrication.

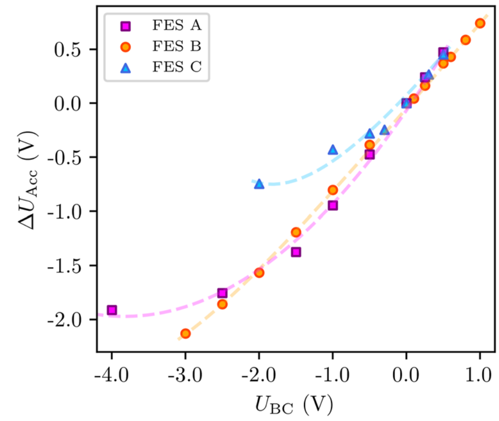

FIG. 4. Shift of the 2DEG accumulation point ΔU_{Acc} as a function of U_{BC} for all three FESs. The dashed lines are guides to the eyes.

IV. CONCLUSION

In conclusion, we have demonstrated that the biased cooling of undoped QW heterostructures creates a static electric field that superimposes on any gate action at the device operation temperature of 1.5 K. While the magnitude of the static electric field scales with the biased cooling voltage U_{BC} applied at room temperature, it is not modified by the top gate voltage U_{TG} action at operation temperature. As a result, the accumulation voltage U_{Acc} of the 2DEG is reproducibly tunable with U_{BC}, allowing U_{Acc} to be set to be positive as well as negative. The shift of U_{Acc} depends linearly on U_{BC} in a wide range. In addition, the capacitive coupling of the FES at device operation temperature is not modified by biased cooling. As a consequence, the whole linear U_{TG}-characteristic of the 2DEG density n_e can be shifted deterministically. Importantly, the main measurables of the U_{TG}-tuned 2DEG remain unchanged compared to $U_{BC} = 0$ V. We did not detect any correlation of U_{BC} either with the lower and upper bound field-effect tunable density or with the 2DEG mobility within the whole range from $n_{e,lb}$ to $n_{e,ub}$ or with the temporal stability of any chosen $n_e(U_{TG})$ within this density range.

As we discuss in an empirical model, all our experimental observations are consistent with a charge $Q = C_{BC} \cdot U_{BC}$ being created at the dielectric/heterostructure interface at room temperature via the loading or unloading of charge traps. Importantly, the loading and unloading mechanisms are suppressed at the device operation temperature. This sets a contrast to previous experiments in modulation-doped GaAs/AlGaAs QW heterojunctions, where biased cooling has been phenomenologically linked to the presence of dopant-induced defects and to leakage of Schottky gates.[15–20] In addition, the charge is homogeneously distributed, such that it does neither impact $n_{e,lb}$, nor the 2DEG mobility or $n_{e,ub}$. Notably, the mechanism is qualitatively identical, although the three investigated FESs differ (see Table I). In particular, the absence or the presence of a Si cap at the dielectric/heterostructure interface does not impact the mechanism.

Our model should apply to any undoped semiconductor heterostructure and confirm recent signatures observed in the Coulomb blockade regime.[23] The ability to shift the operation range of the FES deterministically and reproducibly without affecting the quality features of the 2DEG represents an interesting additional degree of freedom for optimization of gate operation windows. It, for example, allows us to shift "normally on" devices to a "normally off" operation regime.[14] It has also been shown to allow avoiding initializations of 2DEG in metastable capacitive coupling[14] or leakage regimes in Coulomb blockade devices with integrated charge sensors.[22] Applying the biased cooling effect does not require to cycle the device at room temperature. It is sufficient to apply U_{BC} above the freeze out temperature of the heterostructure to induce the loading of Q at the interface.

SUPPLEMENTARY MATERIAL

The supplementary material contains additional data on the density tunability of FES B and FES C.

ACKNOWLEDGMENTS

We acknowledge the financial support of the Deutsche Forschungsgemeinschaft (DFG, German Research Foundation) via Project-ID No. 289786932 (BO 3140/4-2). This work was part of the joint project QUASAR "Halbleiter-Quantenprozessor mit shuttlingbasierter skalierbarer Architektur" (FKZ: 13N15658) and is supported by the German Federal Ministry of Education and Research (BMBF). The research is also part of the Munich Quantum Valley, which is supported by the Bavarian state government with funds from the Hightech Agenda Bavaria.

AUTHOR DECLARATIONS

Conflict of Interest

The authors have no conflicts to disclose.

Author Contributions

Laura K. Diebel: Conceptualization (equal); Data curation (equal); Formal analysis (equal); Investigation (equal); Methodology (equal); Validation (equal); Visualization (equal); Writing – original draft (equal); Writing – review & editing (equal). **Lukas G. Zinkl**: Data curation (equal); Formal analysis (equal); Investigation (equal); Visualization (equal); Writing – original draft (supporting). **Andreas Hötzinger**: Data curation (supporting); Investigation (supporting). **Felix Reichmann**: Resources (equal); Writing – review & editing (supporting). **Marco Lisker**: Resources (equal); Writing – review & editing (supporting). **Yuji Yamamoto**: Resources (equal); Writing – review & editing (supporting). **Dominique Bougeard**: Conceptualization (equal); Funding acquisition (equal); Methodology (equal); Resources (equal); Supervision (equal); Writing – original draft (equal); Writing – review & editing (equal).

DATA AVAILABILITY

The data that support the findings of this study are available from the corresponding author upon reasonable request.

REFERENCES

[1] R. Hanson, L. P. Kouwenhoven, J. R. Petta, S. Tarucha, and L. M. K. Vandersypen, "Spins in few-electron quantum dots," Rev. Mod. Phys. **79**, 1217 (2007).

[2] A. Manchon, H. C. Koo, J. Nitta, S. M. Frolov, and R. A. Duine, "New perspectives for Rashba spin–orbit coupling," Nat. Mater. **14**, 871–882 (2015).

[3] G. Scappucci, C. Kloeffel, F. A. Zwanenburg, D. Loss, M. Myronov, J.-J. Zhang, S. de Franceschi, G. Katsaros, and M. Veldhorst, "The germanium quantum information route," Nat. Rev. Mater. **6**, 926 (2020).

[4] K. Flensberg, F. von Oppen, and A. Stern, "Engineered platforms for topological superconductivity and Majorana zero modes," Nat. Rev. Mater. **6**, 944 (2021).

[5] A. P. M. Place, L. V. H. Rodgers, P. Mundada, B. M. Smitham, M. Fitzpatrick, Z. Leng, A. Premkumar, J. Bryon, A. Vrajitoarea, S. Sussman, G. Cheng, T. Madhavan, H. K. Babla, X. H. Le, Y. Gang, B. Jäck, A. Gyenis, N. Yao, R. J. Cava, N. P. de Leon, and A. A. Houck, "New material platform for superconducting transmon qubits with coherence times exceeding 0.3 milliseconds," Nat. Commun. **12**, 1779 (2021).

[6] D. Thureja, A. Imamoglu, T. Smoleński, I. Amelio, A. Popert, T. Chervy, X. Lu, S. Liu, K. Barmak, K. Watanabe, T. Taniguchi, D. J. Norris, M. Kroner, and P. A. Murthy, "Electrically tunable quantum confinement of neutral excitons," Nature **606**, 298 (2022).

[7] E. J. Connors, J. J. Nelson, H. Qiao, L. F. Edge, and J. M. Nichol, "Low-frequency charge noise in Si/SiGe quantum dots," Phys. Rev. B **100**, 165305 (2019).

[8] T. Struck, A. Hollmann, F. Schauer, O. Fedorets, A. Schmidbauer, K. Sawano, H. Riemann, N. V. Abrosimov, Ł. Cywiński, D. Bougeard, and L. R. Schreiber, "Low-frequency spin qubit energy splitting noise in highly purified ^{28}Si/SiGe," npj Quantum Inf. **6**, 40 (2020).

[9] L. Kranz, S. K. Gorman, B. Thorgrimsson, Y. He, D. Keith, J. G. Keizer, and M. Y. Simmons, "Exploiting a single-crystal environment to minimize the charge noise on qubits in silicon," Adv. Mater. **32**, 2003361 (2020).

[10] D. Degli Esposti, B. Paquelet Wuetz, V. Fezzi, M. Lodari, A. Sammak, and G. Scappucci, "Wafer-scale low-disorder 2DEG in ^{28}Si/SiGe without an epitaxial Si cap," Appl. Phys. Lett. **120**, 184003 (2022).

[11] B. Paquelet Wuetz, D. Degli Esposti, A. M. J. Zwerver, S. V. Amitonov, M. Botifoll, J. Arbiol, L. M. K. Vandersypen, M. Russ, G. Scappucci, and G. Scappucci, "Reducing charge noise in quantum dots by using thin silicon quantum wells," Nat. Commun. **14**, 1385 (2023).

[12] M. Meyer, C. Déprez, T. R. van Abswoude, I. N. Meijer, D. Liu, C.-A. Wang, S. Karwal, S. Oosterhout, F. Borsoi, A. Sammak, N. W. Hendrickx, G. Scappucci, and M. Veldhorst, "Electrical control of uniformity in quantum dot devices," Nano Lett. **23**, 2522 (2023).

[13] L. Massai, B. Hetényi, M. Mergenthaler, F. J. Schupp, L. Sommer, S. Paredes, S. W. Bedell, P. Harvey-Collard, G. Salis, A. Fuhrer, and N. W. Hendrickx, "Impact

of interface traps on charge noise and low-density transport properties in Ge/SiGe heterostructures," Commun. Mater. **5**, 151 (2024).
[14]M. Prager, M. Trottmann, J. Schmidt, L. Ebnet, D. Schuh, and D. Bougeard, "Gating of two-dimensional electron systems in (In,Ga)As/(In,Al)As heterostructures: The role of intrinsic (In,Al)As deep donor defects," Phys. Rev. Appl. **16**, 064028 (2021).
[15]A. R. Long, J. H. Davies, M. Kinsler, S. Vallis, and M. C. Holland, "A simple model for the characteristics of GaAs/AlGaAs modulation-doped devices," Semicond. Sci. Technol. **8**, 1581 (1993).
[16]E. Buks, M. Heiblum, and H. Shtrikman, "Correlated charged donors and strong mobility enhancement in a two-dimensional electron gas," Phys. Rev. B **49**, 14790 (1994).
[17]E. Buks, M. Heiblum, Y. Levinson, and H. Shtrikman, "Scattering of a two-dimensional electron gas by a correlated system of ionized donors," Semicond. Sci. Technol. **9**, 2031 (1994).
[18]P. T. Coleridge, "Correlation lengths for scattering potentials in two-dimensional electron gases," Semicond. Sci. Technol. **12**, 22 (1997).
[19]M. Pioro-Ladrière, J. H. Davies, A. R. Long, A. S. Sachrajda, L. Gaudreau, P. Zawadzki, J. Lapointe, J. Gupta, Z. Wasilewski, and S. Studenikin, "Origin of switching noise in GaAs/$Al_xGa_{1-x}As$ lateral gated devices," Phys. Rev. B **72**, 115331 (2005).
[20]C. Buizert, F. H. L. Koppens, M. Pioro-Ladriére, H.-P. Tranitz, I. T. Vink, S. Tarucha, W. Wegscheider, and L. M. K. Vandersypen, "*In situ* reduction of charge noise in GaAs/$Al_xGa_{1-x}As$ Schottky-gated devices," Phys. Rev. Lett. **101**, 226603 (2008).
[21]B. M. Maune, M. G. Borselli, B. Huang, T. D. Ladd, P. W. Deelman, K. S. Holabird, A. A. Kiselev, I. Alvarado-Rodriguez, R. S. Ross, A. E. Schmitz, M. Sokolich, C. A. Watson, M. F. Gyure, and A. T. Hunter, "Coherent singlet-triplet oscillations in a silicon-based double quantum dot," Nature **481**, 344 (2012).
[22]E. Kammerloher, A. Schmidbauer, L. Diebel, I. Seidler, M. Neul, M. Künne, A. Ludwig, J. Ritzmann, A. Wieck, D. Bougeard, L. R. Schreiber, and H. Bluhm, "Sensing dot with high output swing for scalable baseband readout of spin qubits," Phys. Rev. Appl. **22**, 024044 (2024).
[23]J. Ferrero, T. Koch, S. Vogel, D. Schroller, V. Adam, R. Xue, I. Seidler, L. R. Schreiber, H. Bluhm, and W. Wernsdorfer, "Noise reduction by bias cooling in gated Si/Si_xGe_{1-x} quantum dots," Appl. Phys. Lett. **124**, 204002 (2024).
[24]T. M. Lu, D. C. Tsui, C.-H. Lee, and C. W. Liu, "Observation of two-dimensional electron gas in a Si quantum well with mobility of 1.6×10^6 cm^2/Vs," Appl. Phys. Lett. **94**, 182102 (2009).
[25]M. Neul, I. V. Sprave, L. K. Diebel, L. G. Zinkl, F. Fuchs, Y. Yamamoto, C. Vedder, D. Bougeard, and L. R. Schreiber, "Local laser-induced solid-phase recrystallization of phosphorus-implanted Si/SiGe heterostructures for contacts below 4.2 K," Phys. Rev. Mater. **8**, 043801 (2024).
[26]A. Mistroni, F. Reichmann, Y. Yamamoto, M. H. Zöllner, G. Capellini, L. Diebel, D. Bougeard, and M. Lisker, "Low disorder and high Mobility 2DEG in Si/SiGe fabricated in 200 mm BiCMOS pilot line," ECS Trans. **114**, 123 (2024).
[27]T. M. Lu, C.-H. Lee, S.-H. Huang, D. C. Tsui, and C. W. Liu, "Upper limit of two-dimensional electron density in enhancement-mode Si/SiGe heterostructure field-effect transistors," Appl. Phys. Lett. **99**, 153510 (2011).
[28]A. Wild, J. Kierig, J. Sailer, J. W. Ager, E. E. Haller, G. Abstreiter, S. Ludwig, and D. Bougeard, "Few electron double quantum dot in an isotopically purified ^{28}Si quantum well," Appl. Phys. Lett. **100**, 143110 (2012).
[29]C.-T. Huang, J.-Y. Li, K. S. Chou, and J. C. Sturm, "Screening of remote charge scattering sites from the oxide/silicon interface of strained Si two-dimensional electron gases by an intermediate tunable shielding electron layer," Appl. Phys. Lett. **104**, 243510 (2014).
[30]D. Laroche, S.-H. Huang, E. Nielsen, Y. Chuang, J.-Y. Li, C. W. Liu, and T. M. Lu, "Scattering mechanisms in shallow undoped Si/SiGe quantum wells," AIP Adv. **5**, 107106 (2015).
[31]X. Mi, T. M. Hazard, C. Payette, K. Wang, D. M. Zajac, J. V. Cady, and J. R. Petta, "Magnetotransport studies of mobility limiting mechanisms in undoped Si/SiGe heterostructures," Phys. Rev. B **92**, 035304 (2015).